Controlling Brownian motion of single protein molecules and single fluorophores in aqueous buffer

Adam E. Cohen[1*], **W. E. Moerner**[1]

[1] *Dept. of Chemistry, Stanford University, Stanford, CA 94305*
[*] *Current address: Depts. of Chemistry and Chemical Biology and Physics, Harvard University, Cambridge, MA 02138*
cohen@chemistry.harvard.edu

Abstract: We present an Anti-Brownian Electrokinetic trap (ABEL trap) capable of trapping individual fluorescently labeled protein molecules in aqueous buffer. The ABEL trap operates by tracking the Brownian motion of a single fluorescent particle in solution, and applying a time-dependent electric field designed to induce an electrokinetic drift that cancels the Brownian motion. The trapping strength of the ABEL trap is limited by the latency of the feedback loop. In previous versions of the trap, this latency was set by the finite frame rate of the camera used for video-tracking. In the present system, the motion of the particle is tracked entirely in hardware (without a camera or image-processing software) using a rapidly rotating laser focus and lock-in detection. The feedback latency is set by the finite rate of arrival of photons. We demonstrate trapping of individual molecules of the protein GroEL in buffer, and we show confinement of single fluorophores of the dye Cy3 in water.

OCIS codes: (180.2520) Microscopy: Fluorescence microscopy; (180.5810) Microscopy: Scanning microscopy;(300.6280) Spectroscopy : Spectroscopy, fluorescence and luminescence

References and links

1. R. S. Van Dyck, P. B. Schwinberg, and H. G. Dehmelt, "New high-precision comparison of electron and positron g factors," Phys. Rev. Lett. **59**, 26–29 (1987).
2. M. B. Comisarow and A. G. Marshall, "Frequency-sweep Fourier transform ion cyclotron resonance spectroscopy," Chem. Phys. Lett. **26**, 489–490 (1974).
3. J. Enderlein, "Tracking of fluorescent molecules diffusing within membranes," Appl. Phys. B **71**, 773–777 (2000).
4. A. J. Berglund and H. Mabuchi, "Feedback controller design for tracking a single fluorescent molecule," Appl. Phys. B **78**, 653–659 (2004).
5. A. J. Berglund and H. Mabuchi, "Tracking-FCS: Fluorescence correlation spectroscopy of individual particles," Opt. Express **13**, 8069–8082 (2005).
6. A. J. Berglund and H. Mabuchi, "Performance bounds on single-particle tracking by fluorescence modulation," Appl. Phys. B **83**, 127–133 (2006).
7. A. J. Berglund, K. McHale, and H. Mabuchi, "Fluctuations in closed-loop fluorescent particle tracking," Opt. Express **15**, 7752–7773 (2007).
8. D. Montiel, H. Cang, and H. Yang, "Quantitative characterization of changes in dynamical behavior for single-particle tracking studies," J. Phys. Chem. B (2006).
9. H. Cang, C. M. Wong, C. S. Xu, A. H. Rizvi, and H. Yang, "Confocal three dimensional tracking of a single nanoparticle with concurrent spectroscopic readouts," Appl. Phys. Lett. **88**, 223,901 (2006).
10. C. S. Xu, H. Cang, D. Montiel, and H. Yang, "Rapid and Quantitative Sizing of Nanoparticles Using Three-Dimensional Single-Particle Tracking," J. Phys. Chem. C **111**, 32–35 (2007).

#91292 - $15.00 USD Received 3 Jan 2008; revised 23 Apr 2008; accepted 30 Apr 2008; published 1 May 2008

11. S. Chaudhary and B. Shapiro, "Arbitrary steering of multiple particles independently in an electro-osmotically driven microfluidic system," IEEE Transactions on Control Systems Technology pp. 669–680 (2005).
12. M. Armani, S. Chaudhary, R. Probst, and B. Shapiro, "Using feedback control and micro-fluidics to steer individual particles," Journal of Microelectromechanical Systems (JMEMS) **15**, 945–956.
13. A. E. Cohen and W. E. Moerner, "Method for trapping and manipulating nanoscale objects in solution," Appl. Phys. Lett. **86**, 093,109 (2005).
14. A. E. Cohen and W. E. Moerner, "Suppressing Brownian motion of individual biomolecules in solution," Proc. Natl. Acad. Sci. USA **103**, 4362–4365 (2006).
15. A. E. Cohen and W. E. Moerner, "Internal mechanical response of a polymer in solution," Phys. Rev. Lett. **98**, 116,001 (2007).
16. A. E. Cohen and W. E. Moerner, "Principal Components Analysis of shape fluctuations of single DNA molecules," Proc. Natl. Acad. Sci. USA **104**, 12,622–12,627 (2007).
17. A. E. Cohen, "Control of nanoparticles with arbitrary two-dimensional force fields," Phys. Rev. Lett. **94**, 118,102 (2005).
18. A. E. Cohen, "Trapping and manipulating single molecules in solution," Ph.D. thesis, Stanford University (2007). Https://www2.lsdiv.harvard.edu/labs/cohen/Publications/AEC_Thesis2_OneSided.pdf.
19. A. E. Cohen and W. E. Moerner, "An all-glass microfluidic cell for the ABEL trap: fabrication and modeling," Proc. SPIE **5930**, 191–198 (2005).
20. H. Y. Wang, R. S. Foote, S. C. Jacobson, J. H. Schneibel, and J. M. Ramsey, "Low temperature bonding for microfabrication of chemical analysis devices," Sensors and Actuators B **45**, 199–207 (1997).
21. Z. Ding, G. Lai, T. Sakakibara, and S. Shinohara, "Determination of the spring constant of an optical trap by external sinusoidal excitation and lock-in detection," J. Appl. Phys. **88**, 737–741 (2000).
22. S. S. Sommer and J. E. Cohen, "The size distributions of proteins, mRNA, and nuclear RNA," J. Molec. Evol. **15**, 37–57 (1980).
23. S. Ghaemmaghami, W. Huh, K. Bower, R. W. Howson, A. Belle, N. Dephoure, E. K. O'Shea, and J. S. Weissman, "Global analysis of protein expression in yeast," Nature **425**, 737–741 (2003).

1. Introduction

The invention of traps for individual atoms and molecules in the gas phase led to new physical measurements (e.g. of the anomalous magnetic moment of the electron[1]), and new analytical techniques (e.g. ion cyclotron mass spectrometry[2]). Molecules in solution show much more complex behavior than molecules in the gas phase, but until now there have not existed devices capable of trapping single molecules in aqueous buffer. To address this issue we designed and built an Anti-Brownian Electrokinetic trap (ABEL trap) that grabs and holds single proteins in water at room temperature. We also used this device to temporarily confine single fluorophores of the dye Cy3 (molecular weight ~ 500), although these dye molecules were not stably trapped for long times. These fluorophores have a mass smaller by a factor of 6×10^3 than that of the smallest objects previously trapped under comparable conditions.

In recent years there has been much interest in designing systems to track[3, 4, 5, 6, 7, 8, 9, 10] and trap[11, 12, 13, 14] small particles in solution. These systems all rely on observing the motion of a particle, and then canceling this motion either by translating the sample stage or by applying electrokinetic forces to the particle. The latency of the feedback loop determines the minimum size of particle that can be trapped and the minimum area to which a particle can be trapped. In the mechanical feedback systems, this latency is typically limited by the inertia of the feedback stage; in the electrokinetic systems the response of the particle to an applied field occurs faster than our 40 kHz measurement bandwidth, so the latency is limited by the bandwidth of the tracking system.

In the ABEL trap a small particle diffuses in a pancake-shaped fluid element defined by a nanofluidic cell. A fluorescence tracking system follows the two-dimensional Brownian motion of the particle, and a feedback system applies voltages that induce a combined electrophoretic and electroosmotic drift that cancels the Brownian motion. An earlier version of the ABEL trap used video tracking and computer-controlled feedback to achieve a latency of 4.5 ms, principally due to the 300 Hz maximum frame-rate of the camera. This latency set a lower bound of 20 nm on the diameter of objects that could be trapped in water (although smaller

#91292 - $15.00 USD Received 3 Jan 2008; revised 23 Apr 2008; accepted 30 Apr 2008; published 1 May 2008

objects could be trapped by increasing the viscosity of the solution[14]). With this software-based ABEL trap it was possible to observe the shape fluctuations of single DNA molecules in free solution[15, 16] and to control the motion of nanoparticles subject to arbitrary force-fields[17].

The ABEL trap described here has a feedback latency of 25 μs, almost 200 times faster than earlier devices. At detected photon count rates below 40 kHz, feedback is provided on every detected photon, i.e. at the quantum limit on the feedback bandwidth. Our tracking system is a variant of the rotating laser method originally proposed by Enderlein, [3] and first implemented by Berglund and Mabuchi.[4, 5] Figure 1 shows a schematic of the apparatus. The essential idea is that a small laser spot rotates in a circle at a high speed around the object to be trapped. If the object moves off-center, there is a modulation of the fluorescence intensity at the rotation-rate of the laser beam; the phase of this modulation indicates the direction in which the particle moved. The positional information is used to generate a pair of feedback voltages which cause the particle to return to the center of the trap.

This paper is organized as follows. Section 2 describes the optoelectronic aspects of the trap; Section 3 summarizes the design and construction of the nanofluidic cell; Section 4 presents the characterization and application of the hardware-feedback ABEL trap.

2. Illumination train

2.1. Acousto-optic deflectors

The centerpiece of the tracking subsystem is an X-Y acousto-optic beam deflector (AOBD; Neos Technologies, Melbourne FL). The AOBD consists of a pair of shear-wave TeO_2 crystals, each with a 5 mm aperture, driven with a pair of 40 kHz sinusoids, phased to drive the laser beam in a circular pattern (due to nonuniform propagation delays in the AOBD crystals, the drive signals typically have a phase shift $\neq 90^\circ$). Ideally one would like the rotation frequency of the laser beam to be as high as possible. The rotation frequency sets the maximum bandwidth of the feedback loop, but if the rotation frequency is higher than the maximum photon detection rate, then the bandwidth is limited by photon statistics.

The maximum rotation rate of the laser is set by the time for the acoustical wave in the AOBD to cross the laser illumination area. To avoid blurring, the deflection angle must change on a timescale much slower than the transit time, setting a maximum frequency of 40 kHz. Designs based on longitudinal-wave AOBDs or electro-optic beam deflectors may achieve higher rotation rates and thus higher maximum bandwidths.

An additional low-frequency signal from the computer or other source can be added to the AOBD drive voltages. This signal is used to move the trap-position by a small amount in real time. By modulating the position of the trap center one can learn about the electrokinetic mobility of the trapped object (see sec. 4.3).

2.2. Illumination optics

The placement of lenses in the illumination train is a subtle issue subject to several constraints. Inside the trapping region, the laser beam has a width and a divergence angle. Furthermore, the AOBD causes the center of the beam to describe a cone, with its own width in the trapping region and divergence angle. Thus there are four parameters that need to be adjusted for optimal trapping: (beam width w_b, beam divergence θ_b, cone width w_c, cone divergence θ_c, see Fig. 2).

In the limit of a very thin trapping region, the divergence angles of the beam and of the cone are irrelevant; one only has to consider their widths. One wants $w_b \sim w_c$. If $w_c \gg w_b$ then the illumination is annular and particles in the center of the trapping region are not illuminated. If $w_c \ll w_b$ then there is little modulation in the fluorescence intensity as a particle moves away

#91292 - $15.00 USD Received 3 Jan 2008; revised 23 Apr 2008; accepted 30 Apr 2008; published 1 May 2008

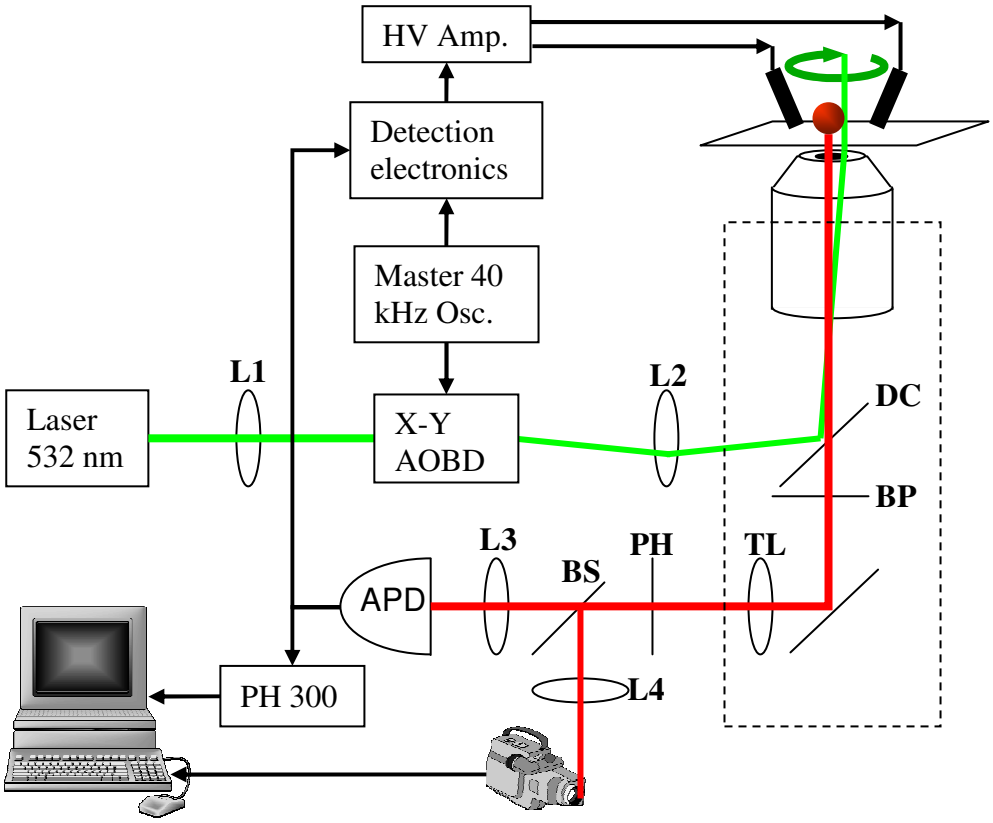

Fig. 1. Schematic of the hardware-feedback ABEL trap. A two-dimensional acousto-optic beam deflector (AOBD) deflects a laser beam in a small circle at 40 kHz. The excitation light reflects of dichroic mirror **DC** and illuminates a particle in the trap. A bandpass filter **BP** blocks scattered excitation light while passing fluorescence. The tube lens **TL** focuses the fluorescence onto a pinhole **PH**, and the fluorescence photons are then detected by an avalanche photodiode (APD). Phase-sensitive detection of individual photons provides a sensitive indicator of the offset between the location of the particle and the center of the trap. A time-correlated single-photon counting module (PH 300) records the arrival time of each photon, and a beamsplitter **BS** diverts a small fraction of the fluorescence light toward a camera.

#91292 - $15.00 USD Received 3 Jan 2008; revised 23 Apr 2008; accepted 30 Apr 2008; published 1 May 2008

from the center. The largest modulation is obtained when the center of revolution coincides with the point of maximum gradient in the intensity of the beam.

Several factors go into choosing an optimal overall size for the illuminated region. Increasing the radius of the illuminated region increases the distance a particle must go before it escapes. This decreases the average force required to set a well-depth of several k_BT, and allows more time for the feedback to catch a particle before it diffuses out of the trap. Thus regardless of whether the trap is limited by feedback latency or feedback strength, larger trapping regions help.

On the other hand, the signal from the particle is proportional to the time-average *intensity* of the excitation, while the background coming from the entire illuminated volume is proportional to the time-average *power*. Thus the signal-to-background ratio (SBR) increases with decreasing illumination area. The background may come from Raman scattering, autofluorescence, laser light leaking through the emission filters, or the presence of other fluorescent particles in the solution. This last issue is particularly important. The illuminated region sets the capture radius of the trap. The larger this region, the more likely it is that at a given concentration more than one particle will enter the trapping region. Thus to maintain a given trapping time without interference from other fluorescent particles, larger illumination regions require working at lower concentrations. This in turn increases the requirements on sample purity, an important factor when working at picomolar concentrations. We found that a 2 micron diameter illumination region (with a 0.75 μm illumination spot) worked well under most conditions.

The question of the two divergence angles, θ_b and θ_c is more subtle. Ideally the beam itself will come to a focus in the trapping region, and will have a confocal length greater than the depth of the trapping region. The confocal length b is given by

$$b = \frac{2\pi w_b^2}{\lambda}, \tag{1}$$

where λ is the wavelength of light and w_b is the radius of the waist. With $w_b = 0.75$ μm we achieve $b = 6.6$ μm with 532 nm light, which is large enough to consider the beam as purely collimated in the trapping region (typical depth $< 1\mu$m). The far-field divergence angle of this beam is

$$\theta_b = \frac{\lambda}{\pi w_b}, \tag{2}$$

which for the scenario we are considering is 13°. We want this beam to propagate purely perpendicular to the trapping plane, i.e. $\theta_c = 0$. Figure 2(a) shows the desired illumination pattern.

Starting with the desired illumination pattern on the right of Fig. 2(b), we now follow the beam from right to left to determine the placement of the optical elements. The 100x objective has a focal length $f_O = 2$ mm. To achieve a convergence angle of 13°, the beam entering the objective should be collimated and have a radius of $2\sin(13^\circ) = 0.45$ mm. Such a beam has a Rayleigh length of 1.2 m, so we can consider it to propagate as a pencil beam on the scale of tens of centimeters. The lens combination **L1,L2** spaced by $f_1 + f_2$ decreases the diameter of the beam emerging from the laser by a factor of f_1/f_2. Our 532 nm 30 mW green laser diode (World Star Tech, Toronto, Canada) generates a beam with a radius of ~ 1 mm, so we want $f_1/f_2 \sim 2$.

The AOBD should change the position at which the beam emerges from the objective, without changing the direction of propagation. This means that the AOBD must change the *angle* of the beam at the back focal plane of the objective, but not its position. Placing lens **L2** a distance $2f_2$ from the back focal plane, and the AOBD another $2f_2$ behind **L2** achieves this goal.

#91292 - $15.00 USD Received 3 Jan 2008; revised 23 Apr 2008; accepted 30 Apr 2008; published 1 May 2008

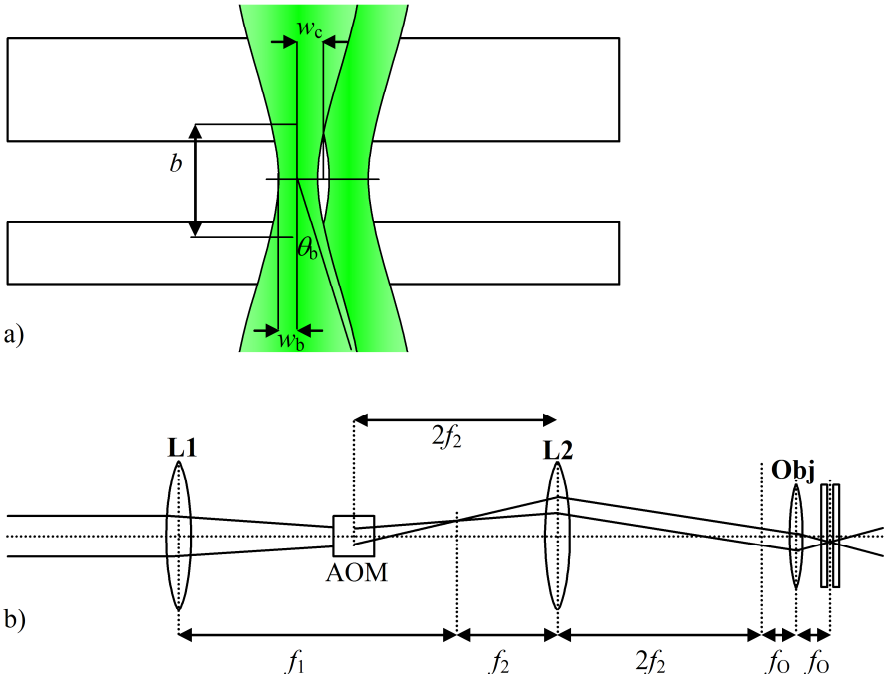

Fig. 2. Excitation path for the hardware-feedback ABEL trap. a) Geometry of the excitation beam in the trapping region. We want the beam to propagate perpendicular to the trapping plane, and to have a confocal depth much greater than the depth of the trapping region. b) Optical setup to create the beam pictured in (a). Lens **L1** has a focal length of $f_1 = 40$ cm and lens **L2** has a focal length of $f_2 = 18$ cm.

2.3. Detection optics

The collection optics are shown in Fig. 3. Fluorescence from the particle is collected by the objective and passes through a dichroic longpass filter (545DCLP Chroma), followed by two bandpass emission filters (550LP, Chroma). The tube lens, **TL**, has a focal length of $f_{TL} = 200$ mm and focuses the image onto a 200 μm pinhole (corresponding to 2 μm in the sample plane). A 90:10 (R:T) beamsplitter directs the bulk of the light onto the APD, while allowing some light to reach the EMCCD camera which is used for recording pictures of trapped molecules.

A 20x air objective **L3** focuses the light on the APD (SPCM-CD 2801, Perkin Elmer, 250 dark counts/sec). Lens **L4** has a focal length of $f_4 = 10$ cm and focuses the light onto the camera (Cascade 512B, Roper Scientific). The images from the camera are recorded on a computer. The TTL pulses from the APD go to a 1:3 TTL fanout box. One output of the fanout goes to a PicoHarp 300 Time-Correlated Single Photon Counting (TCSPC) module (Picoquant, Berlin, Germany), and the other output goes to the demodulation electronics.

2.4. Photon-by-photon feedback

In our initial experiments we used a vector lock-in amplifier (SR-844, Stanford Research Systems, Sunnyvale, California) for the demodulation. The raw signal from the APD went into the input channel, and a 40 kHz reference square wave into the reference channel. Adjusting the "phase" knob on the lock-in rotated the x and y output channels to correspond to the x and y displacements of the trapped particle. While this approach worked, it introduced an unnecessary

#91292 - $15.00 USD Received 3 Jan 2008; revised 23 Apr 2008; accepted 30 Apr 2008; published 1 May 2008

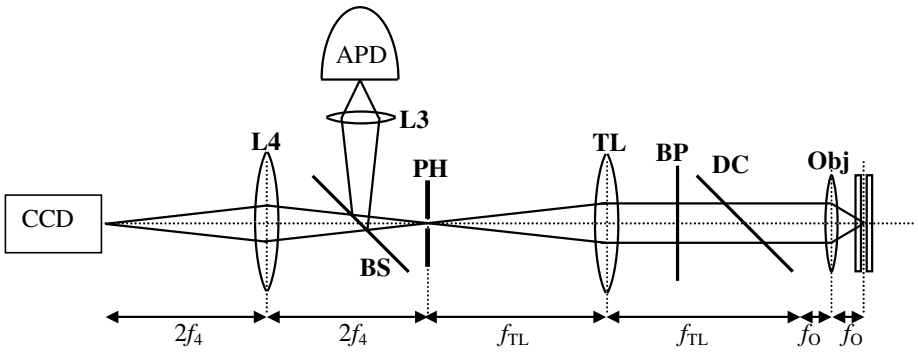

Fig. 3. Detection path for the hardware-feedback ABEL trap.

latency due to the propagation time of the signal through the lock-in electronics. Even with the shortest possible integration time of 100 μs, the device had a fixed system delay of $\sim$ 150 μs, leading to a total feedback latency of 250 μs, or 10 times the laser rotation period.

To reach the ultimate feedback bandwidth allowed by the 40 kHz AOBD frequency, we built custom demodulation electronics based around a pair of AD8182 high speed analog switches. These switches passed samples of a 40 kHz sine and cosine, sampled at the times of the pulses delivered by the APD. Thus the output voltages from the pair of analog switches represented a vector indicating the position of the laser beam (and hence the position of the particle) at the instant of each detected photon. The outputs of the analog switches passed through a filter which blocked components of the signal at 40 kHz and all harmonics. The purpose of this filter was to remove noise induced by the rotation of the laser beam, which otherwise might have lead to a *rotation* of the trapped particle. The filtered signal was amplified and applied to the cell as the feedback voltages. A more detailed description of the electronics, including circuit diagrams, is provided in Ref.[18].

3. Fused silica sample cell

The hardware-feedback ABEL trap is much more sensitive to background autofluorescence than the software ABEL trap because the hardware setup collects *all* the photons from the 2 μm-diameter trapping region onto a single APD pixel. Also the hardware-feedback ABEL trap is fast enough to trap very small objects, which tend to be dim and thus have a low SBR. We found that the glass microfluidic cells used in the software trap[19] had too much autofluorescence to be used in the hardware trap. When excited at 532 nm, fused silica has $\sim 40\times$ less autofluorescence than Corning 7740 borosilicate glass. Unfortunately, fused silica is a difficult material to work with: it is harder than most other materials and resistant to most dry or wet etching procedures.

Fused silica microfluidic cells were made in the Stanford Nanofabrication Facility through a variant of the process we previously used to make glass cells.[19] Fused silica wafers were coated with a layer of polycrystalline Si using low-pressure chemical vapor deposition (LP-CVD). A pattern of channels (Fig. 4(a), dark in the inset) connecting the feedback electrodes to the trapping region was created in photoresist, transferred into the Si via a SF_6 reactive ion etch (RIE), and then ~ 20 μm into the silica via a 6:1 buffered oxide etch (BOE) lasting several hours (the etch rate varies, so it is necessary to check the progress periodically using a stylus profilometer).

The trapping region with z thickness of 400 nm was created in a second step of photolithography. The pattern was transferred into the Si hard-mask via a SF_6 RIE, and then transferred

#91292 - $15.00 USD Received 3 Jan 2008; revised 23 Apr 2008; accepted 30 Apr 2008; published 1 May 2008

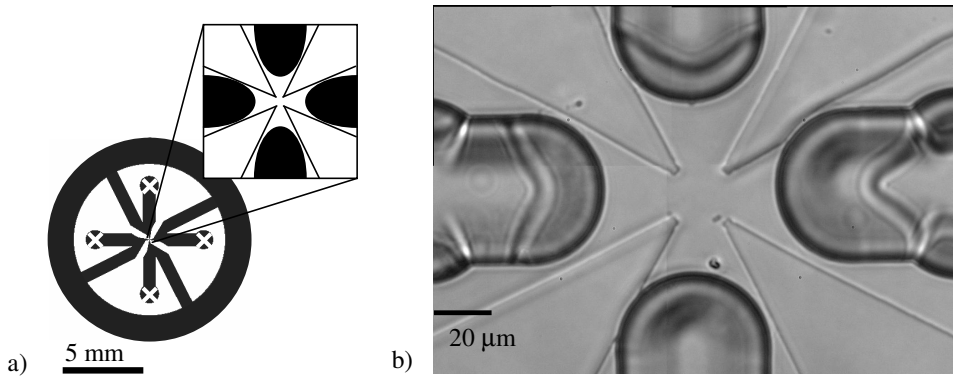

Fig. 4. Fused silica microfluidic cell for the hardware-feedback ABEL trap. a) Macroscopic layout of the deep channels. The annular channel equalizes the hydrostatic pressure in the four arms of the trap, eliminating pressure-driven flows through the trapping region. b) Trapping region. The ends of the deep channels extend from the edges of the image. The wedges jutting from the corners are raised ~ 400 nm above the trapping region and set the depth of the trapping region. These wedges also act to focus the electric field into the center of the trapping region.

~ 400 nm into the silica via a brief etch in 6:1 BOE. The remainder of the Si was then stripped using an SF_6 RIE etch. Through-holes were drilled in the fused silica to provide access for the feedback electrodes, and then the finished chips were bonded to 170 μm-thick fused silica coverslips using the silicate bonding procedure of Ramsey *et al.*[20]. Figure 4(b) shows the center of the trapping region in the fused silica cell.

4. Results

4.1. Characterization of the trap

One of the challenges of working with the hardware-feedback ABEL trap is that the system is very sensitive to the optical alignment and to small phase shifts in the electronics. These sources of error are not simple to detect or to diagnose. To aid with troubleshooting and calibration, we built an additional subsystem for scanning a fixed fluorescent bead through the trapping region. The scanning was performed using a three-axis piezoelectric stage (Physik Instrumente, Karlsruhe, Germany), controlled by home-made software written in Visual Basic. Figure 5 shows a typical calibration scan, made using a 100 nm bead and a 400 μm pinhole (corresponding to 4 μm in the sample plane. From Fig. 5 we see that the average photon count rate is relatively independent of the position of the bead within the trapping region and that the feedback voltages indicate the x,y position of the bead and are relatively independent of its z position.

How accurate is the hardware tracking system? Clearly one can obtain a better estimate of the position of a stationary particle by averaging for a longer time. Higher photon count rates also improve accuracy. We seek a measure that is independent of integration time or photon count rate, and depends purely on the geometry of the optical system. This is achieved by calculating the resolution times *square-root photons detected*. The units of resolution are $[R] = \mu\text{m}\sqrt{N}$, where N is the total number of photons detected in some interval. Given R, one can calculate the resolution for any given integration time and photon count rate. In practice the resolution might be degraded by nonideal behavior of the APD at high count rates or by low-frequency drift in the alignment of the optics.

Figure 6 illustrates the procedure for obtaining R. A linear sweep of a bead through the

#91292 - $15.00 USD Received 3 Jan 2008; revised 23 Apr 2008; accepted 30 Apr 2008; published 1 May 2008

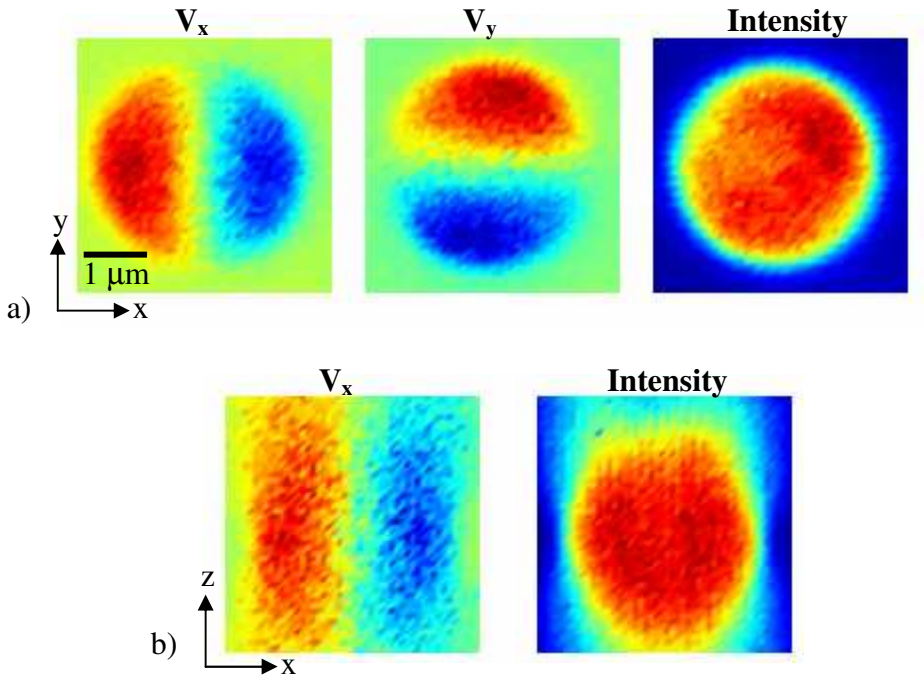

Fig. 5. Calibration of the ABEL trap performed by scanning a fixed 100 nm fluorescent bead through the trapping region. a) Scan in the *x*-*y* plane. The *x* and *y* feedback voltages are proportional to the respective offsets of the particle, and the total photon count rate is independent of the offset. b) Scan in the *x*-*z* plane. The *x* feedback voltage is proportional to the offset, with a gain that does not vary strongly with *z*. Within a large region, the photon count rate is independent of position.

trapping region yields a sensitivity of 0.76 V/μm of displacement in the central part where the response is linear. This number depends on the precise optical alignment, and is proportional to the photon count-rate and the gain in the electronics. Meanwhile, the standard deviation of the mean voltage (averaged over a 25 ms interval) is 49.4 mV, which corresponds to an error in the position measurement of 65 nm. The average count rate during this experiment was 18,500 counts/s, which corresponds to 463 counts in a 25 ms interval. Thus the resolution of the system is $R = 65\ \text{nm} \times \sqrt{463} = 1.4\ \mu\text{m}\sqrt{N}$.

From this analysis we estimate that the accuracy of the tracking system described here is somewhat worse than the diffraction limit of $R \approx 250\ \text{nm}\sqrt{N}$. This is because the beam is expanded to be larger than the diffraction limit. By shrinking the beam one can increase the gradient in intensity in the center of the tracking region, without increasing the overall excitation intensity. Ideally the excitation region will be just large enough to keep the particle from escaping—any extra space only contributes to decreased SBR. Future designs will work toward shrinking the trapping region.

4.2. Trapping beads

Using the hardware-feedback ABEL trap, fluorescent polystyrene beads of diameter 100 nm and 26 nm were trapped so tightly that the video images showed no discernable Brownian motion. Figure 7 shows the results of trapping a 100 nm bead, using the lock-in amplifier to provide feedback. In this experiment the lock-in was set to have an integration time of 100 μs

#91292 - $15.00 USD Received 3 Jan 2008; revised 23 Apr 2008; accepted 30 Apr 2008; published 1 May 2008

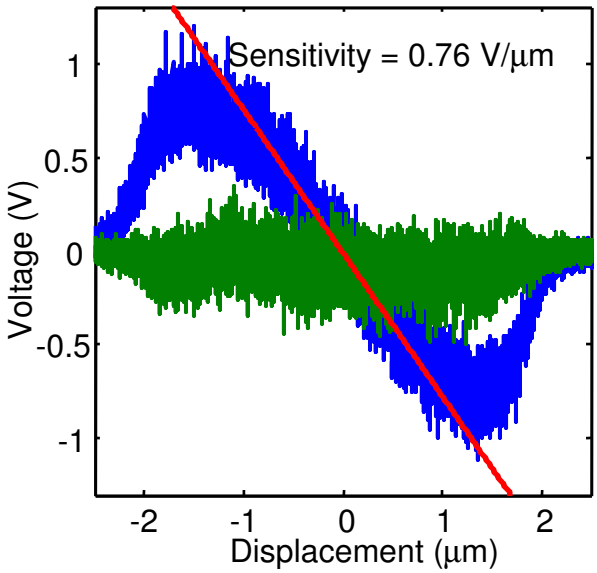

Fig. 6. Feedback voltages as a 100 nm fluorescent bead is scanned through the trapping region. Blue: feedback voltage along the scan axis; green: voltage perpendicular to the scan axis. The sensitivity in this case is 0.76 V/μm and the noise is 1.4 μm$\sqrt{N}$.

and a roll-off of 6 dB/octave. Since the feedback bandwidth (several kHz) is far greater than the video frame rate (92 Hz in this case), it is not possible to determine the amplitude of the position fluctuations from the sequence of video images. However, an upper bound on the position fluctuations may be obtained from the histogram of feedback voltages (Fig. 7(b)). The sensitivity measured with a fixed bead at 12,200 counts/s was 0.49 V/μm; in the experiment the count rate was 119,000 counts/s, yielding a sensitivity of 4.78 V/μm. The voltage fluctuations were 1.12 V r.m.s.; if all of this were due to real fluctuations of the bead as opposed to shot-noise, the position fluctuations would be 230 nm, r.m.s. From the histogram of voltages alone it is not possible to determine how much smaller than 230 nm the position fluctuations of the bead are.

Next we examine the dynamics of the trapped particle. Our only high time-resolution measure of the motion of the particle is the record of feedback voltages used to hold it still. The dynamics of these voltages depend on the properties of the particle, but also on the properties of the feedback system, i.e. the measurement noise and the response function of the feedback electronics. Fortunately all of the variables that do not pertain directly to the particle can be measured off-line in other experiments. For example, we obtained the sensitivity of the trap by scanning a fixed particle through the trapping region. Similarly, we obtained the dynamic response function of the lock-in amplifier by applying a sinusoid at the reference frequency, amplitude modulated with a low-frequency square wave. The response function of the lock-in is the time-derivative of the output voltage measured under these conditions. Figure 7(c) shows the response function of the lock-in. Assuming that the velocity of the particle responds instantaneously to a feedback voltage, the dynamics of the system along one dimension obey:

$$\frac{dx}{dt} = -\mu E(t) + \xi(t) \tag{3}$$

$$E(t) = \int_0^\infty d\tau A G(\tau)[x(t-\tau) + \chi(t-\tau)], \tag{4}$$

#91292 - $15.00 USD Received 3 Jan 2008; revised 23 Apr 2008; accepted 30 Apr 2008; published 1 May 2008

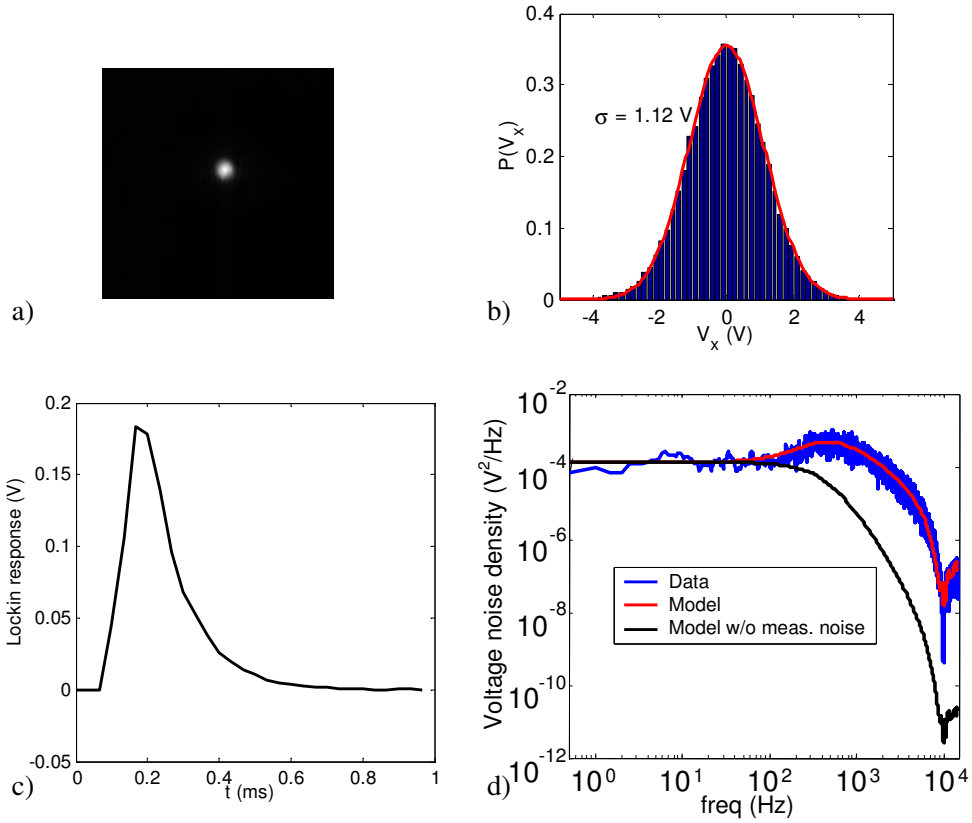

Fig. 7. Trapping of a 100 nm bead in the hardware-feedback ABEL trap. a) Image of a trapped bead obtained by averaging 11 video frames (corresponding to 1 s of data). b) Histogram of voltages applied along the x-axis to keep the bead trapped. c) Impulse response function of the feedback electronics. The latency is dominated by the cruddy SR844 lock-in amplifier. d) Power spectrum of the voltage oscillations (blue), and fits based on Eq. 5 including the effect of measurement noise (red), and without measurement noise (black).

where μ is the mobility, $G(\tau)$ is the impulse response of the lock-in (Fig. 7(c)), A is the gain of the tracking system, ξ is the Brownian noise, and χ is the measurement noise. Based on this model we determine the expected power spectrum of electric field (or voltage) fluctuations:

$$|\tilde{E}(\omega)|^2 = \frac{|A\tilde{G}|^2(|\tilde{\xi}|^2 + \omega^2|\tilde{\chi}|^2)}{\omega^2|1 + \frac{A\mu\tilde{G}}{i\omega}|^2}. \tag{5}$$

Approximating the Brownian fluctuations and the shot noise as statistically independent white noise, the terms $|\tilde{\xi}|^2$ and $|\tilde{\chi}|^2$ can both be replaced by constants. In the absence of other information, this formula has three free parameters: the mobility, the diffusion coefficient (via the Brownian fluctuations), and the measurement noise. If one takes data on a fixed particle of similar brightness, the measurement noise $|\tilde{\chi}|^2$ can be obtained independently, leaving two fitting parameters. Figure 7(d) shows the measured power spectrum of the voltage fluctuations in trapping a 100 nm bead (blue), the fit obtained from Eq. 5 (red), and the fit that would be obtained if measurement noise were neglected (black).

It is simple to solve Eq. 3 for the power spectrum of the *position* fluctuations. Doing this

#91292 - $15.00 USD Received 3 Jan 2008; revised 23 Apr 2008; accepted 30 Apr 2008; published 1 May 2008

yields:

$$|\tilde{x}(\omega)|^2 = \frac{|\tilde{\xi}|^2 + |A\mu\tilde{G}\tilde{\chi}|^2}{\omega^2|(1+\frac{A\mu\tilde{G}}{i\omega})|^2}. \quad (6)$$

Given the parameters obtained from the fit to the voltage fluctuations, and the known tracking sensitivity A, one can evaluate the power spectrum of the position fluctuations. Parseval's identity then yields the total variance in the position of the particle. For the particle in Fig. 7, this procedure yields r.m.s. position fluctuations of 88 nm. By attributing these position fluctuations to thermal energy, we extract an effective spring constant of 5.3×10^{-7} N/m. These numbers are reasonable given what we know about the diffusion coefficient and the latency. A 100 nm sphere has $D = 4.4\ \mu\text{m}^2/\text{s}$. During a delay of $t = 150\ \mu\text{s}$, we expect the sphere to diffuse an r.m.s. distance $\sqrt{2Dt} = 36$ nm. The measured position fluctuations are larger than this estimate because the trap only exerts a finite restoring force (which takes some time to return the particle to the target location) and because measurement noise leads to spurious feedback signals that increase the position fluctuations of the bead. In contrast, a typical optical trap with 100 mW of 532 nm laser light can trap a 1 micron bead (1000 times more massive than the particle trapped here) with a spring constant of 1.8×10^{-6} N/m.[21]

4.3. Manipulating beads

Thermal fluctuations provide all possible sets of perturbations to a trapped particle, so the time series of feedback voltages for a stably trapped particle holds all the information one could hope to obtain about the particle. As we have seen, extracting information from stochastic trajectories can be a complicated task. Often the same information can be obtained far more directly by judiciously modulating the position of the center of the trap. In analogy to optical spectroscopy, there are several quantities beyond the vanilla mobility and diffusion coefficients one might like to measure:

1. Fluctuations in transport coefficients. These fluctuations may arise from conformational fluctuations, interactions with the environment, or ionization events.

2. Dynamic electrokinetic response. The velocity of a particle might depend on past electric fields as well as the instantaneous field due to the finite timescale of electrokinetic and hydrodynamic relaxation processes surrounding a trapped particle.

3. Nonlinear response. At sufficiently high electric fields the proportionality between steady state electric field and drift velocity breaks down, either due to uninteresting effects such as Joule heating, or to interesting effects such as polarization or deformation of the particle.

These quantities are easier to measure if one modulates the target position for the particle, rather than simply holding it near a fixed target.

As mentioned previously, the AOBD driver circuit accepts low frequency x and y voltages to move the center of rotation of the laser in an arbitrary pattern. As long as the modulation is small enough to keep the center of rotation within the field of view defined by the collection pinhole, a trapped particle will follow the indicated pattern.

Figure 8 shows how one can measure the mobility of a trapped 26 nm-diameter particle by stepping the trap center back and forth in a square-wave pattern. In this experiment, the trap center was stepped at 100 Hz, with increasing step sizes. Figure 8(a) shows the the cycle-average response of the feedback voltage. Since the steps of the trap center are uncorrelated with the Brownian motion or the shot noise, these two effects do not contribute to the cycle-averaged response. The area under the voltage vs. time curve is a measure of the impulse the

#91292 - $15.00 USD Received 3 Jan 2008; revised 23 Apr 2008; accepted 30 Apr 2008; published 1 May 2008

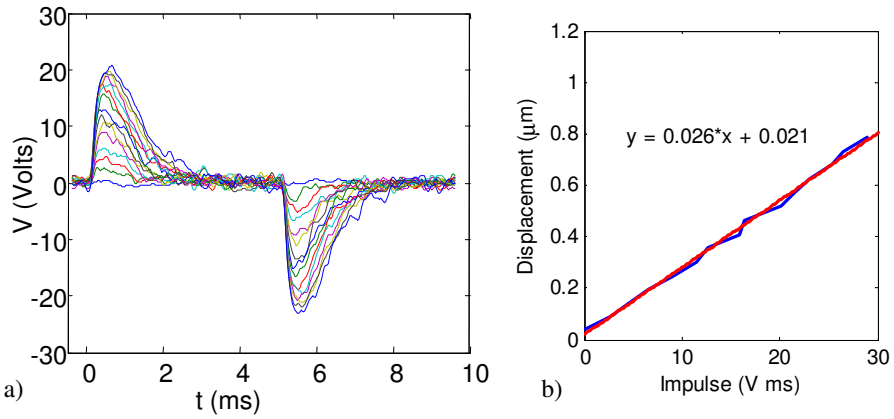

Fig. 8. Measurement of the mobility of a trapped 100 nm bead. a) The position of the trap center was modulated with a square wave of increasing amplitude and the cycle-average voltage was recorded. b) The area under the voltage vs. time curve is proportional to the mobility.

feedback system delivers to the particle. The slope of this impulse as a function of the step size gives the mobility (Fig. 8(b)). So for the bead studied here, the electrokinetic mobility was 26 μm/V·s. The usual units of mobility are μm^2/V·s. We do not know the precise electric field in the trapping region–only the voltages applied–so for simplicity we give mobilities in units of μm/V·s.

The modulation method for measuring mobility has some technical advantages over inferring the mobility from the feedback voltages with a fixed trap center. To derive Eq. 5 for a fixed trap center, we had to assume that the feedback signal was linear in the displacement. Figure 6 shows that this is not true for large displacements. On the other hand, when we modulate the position of the trap center, we know *exactly* how far the center moved (this can be calibrated off-line). Just after the center undergoes a large step, the particle may be displaced far enough to be in the region where the tracking is nonlinear. This nonlinearity affects the shape of the voltage relaxation curve (Fig. 8(a)), but not the area under the curve. Thus the modulation method is insensitive to the details of the illumination pattern and to abberations in the optics (assuming that the velocity of the particle is proportional to the feedback voltage).

4.4. Trapping single molecules of the chaperonin GroEL

To test the trapping strength of the hardware-feedback setup on a nanoscale object, single molecules of fluorescently labeled chaperonins were loaded into the trap. Each GroEL molecule ($\sim$ 800 kDa) was labeled with, on average, 6 molecules of Cy3. Figure 9 shows the results, proving that single molecules were clearly held in the trap for several seconds. Similar molecules were immobilized using software-based feedback[14], but only in a solution of 50% glycerol, which had 6 times the viscosity of water.

4.5. Trapping single molecules of Cy3

A "typical" protein has a diameter of 2.5 nm.[22, 23]. The chaperonin GroEL is much larger, roughly 14 nm by 18 nm. In fact, most of the proteins studied by single-molecule methods are either very large, or interact with something very large, e.g. DNA, actin, cell membrane, etc. This is because the molecule must somehow be immobilized for extended observation. For the ABEL trap to be truly useful, it should be able to trap objects smaller than $\sim$ 2.5 nm in buffer.

#91292 - $15.00 USD Received 3 Jan 2008; revised 23 Apr 2008; accepted 30 Apr 2008; published 1 May 2008

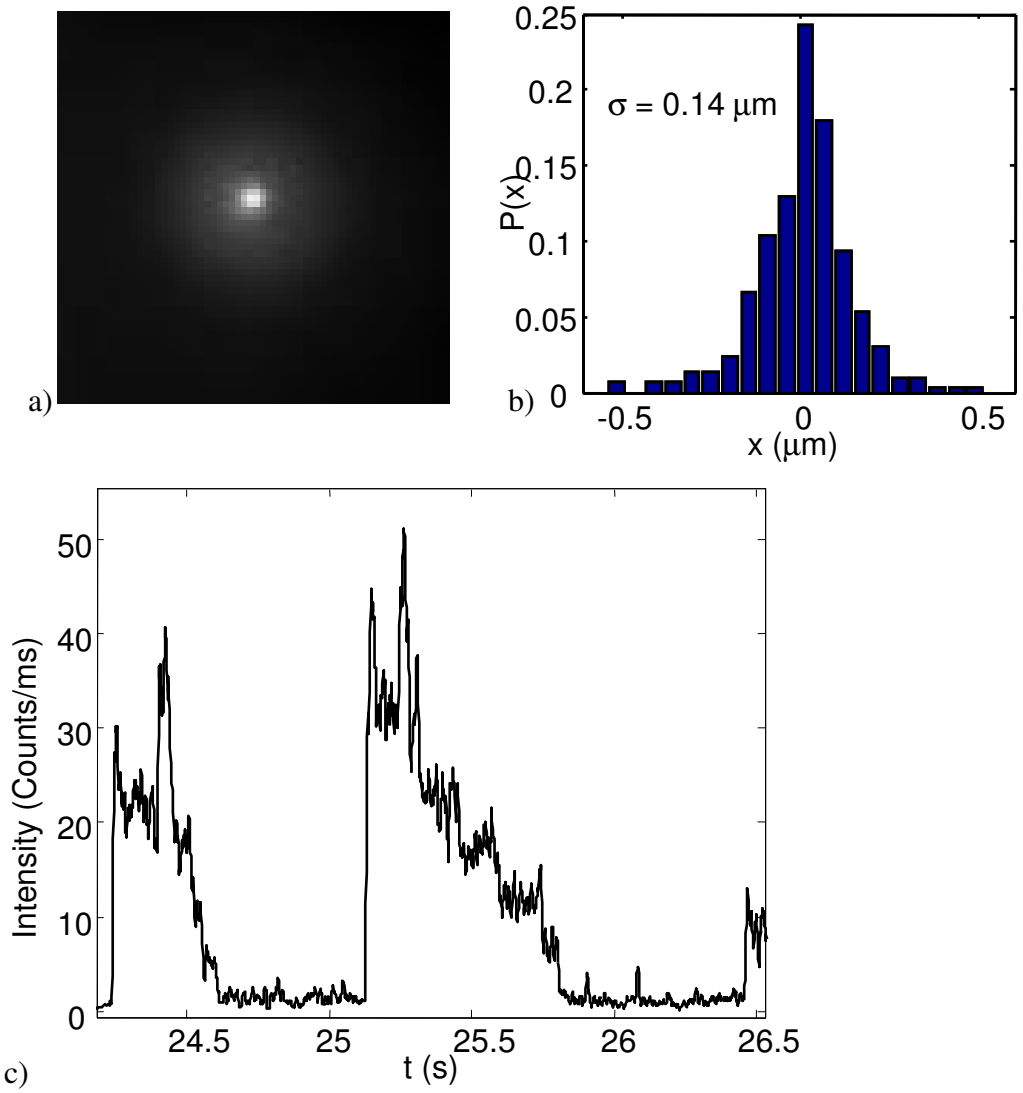

Fig. 9. Trapping of a single chaperonin in buffer. a) Time-lapse image of a single trapped molecule of GroEL (held for $\sim$ 1.7 s). b) Histogram of the displacements of the molecule, extracted from the trajectory of video images. c) Photobleaching time-trace of trapped single molecules of the fluorescently labeled archeal chaperonin MmCpn. Discrete photobleaching steps are clearly visible.

#91292 - $15.00 USD Received 3 Jan 2008; revised 23 Apr 2008; accepted 30 Apr 2008; published 1 May 2008

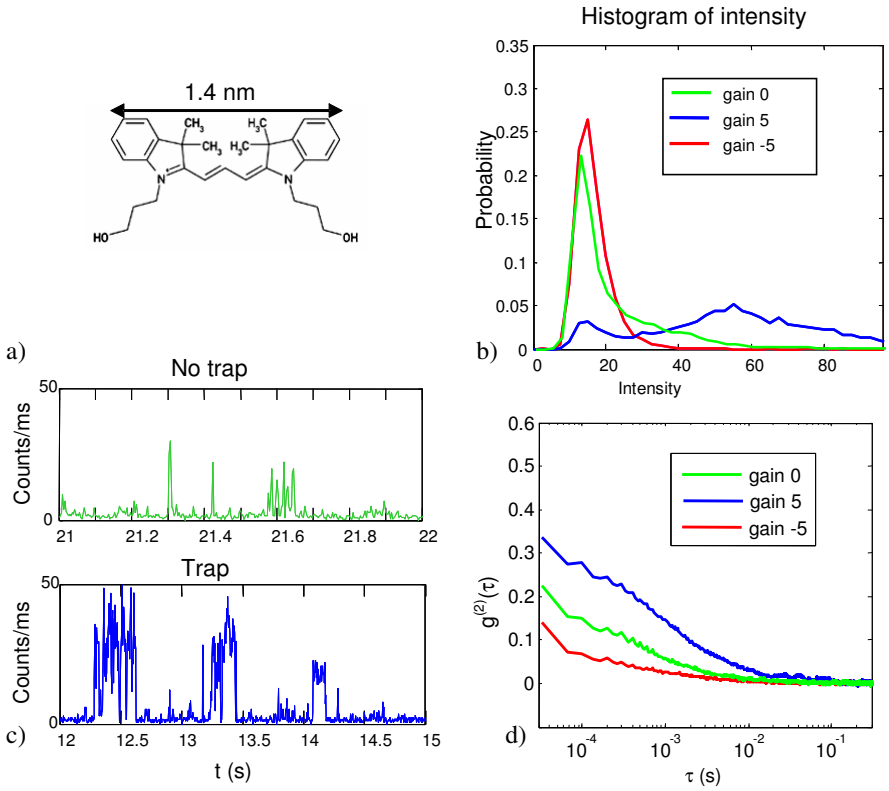

Fig. 10. Trapping of Cy3. a) Molecular structure of Cy3. The molecular weight is 507 g/mol. b) Histogram of count-rates in the trapping region, with no feedback, feedback, and anti-feedback. c) Representative time-traces with and without feedback. d) Autocorrelation of the intensity with no feedback, feedback, and anti-feedback.

The smallest object one could conceive of trapping is a single fluorophore. Except for the rare cases of autofluorescent proteins, any protein held in the ABEL trap would be fluorescently labeled. Thus if one can trap a single fluorophore, one can trap any protein.

The fluorophore Cy3 has a molecular weight of 507, and is roughly 1.4 nm along its longest dimension. Cy3 absorbs in the green, and is relatively photostable in the absence of oxygen. A solution of Cy3-succinimidyl ester was incubated with a 1:2 molar ratio of DTT in order to hydrolyze the succinimide groups. Trapping was performed in an oxygen-scavenging buffer (HEPES (50 mM), glucose (4.5 mg/mL), glucose oxidase (0.43 mg/mL), catalase (72 μg/mL), and β-mercaptoethanol (5 μL/mL)) at a Cy3 concentration of 0.2 nM. HEPES was chosen as the trapping buffer because it is zwitterionic: it contributes very little to the conductivity of the solution, so Joule heating should not be a problem even at high feedback strengths.

We were not able to trap a single Cy3 for an extended time, although Fig. 10 shows that the residence times of single Cy3 molecules in the trap was dramatically enhanced. Figure 10(b) shows histograms of the intensity in the trapping region, with the feedback on, off, and negative. The strong peak at 18 counts/ms is the background signal from scattered laser light, Raman scattering, and autofluorescence. The green trace (no feedback) shows a long tail extending up to 60 counts/ms. This tail is due to fluorophores diffusing in and out of the trapping region. When the feedback is turned on (blue trace) a discrete peak develops centered around 55 counts/ms. This peak corresponds to the intensity from a single fluorophore in the trap.

#91292 - $15.00 USD Received 3 Jan 2008; revised 23 Apr 2008; accepted 30 Apr 2008; published 1 May 2008

As a control experiment, we reversed the sign of the feedback, so any particle in the trapping region received kicks directed radially *outward*. The red curve shows that under these "anti-trapping" conditions, the long tail present in the free-diffusion trace disappeared. Thus it is possible to use the ABEL trap to create a localized *dip* in the concentration of fluorescent molecules.

Figure 10(c) shows typical time-traces of the binned fluorescence intensity with the feedback off and on. The brief bursts in the top panel correspond to molecules diffusing randomly through the trapping region. With the feedback on, the bursts last much longer; some as long as 500 ms. Figure 10(d) shows the autocorrelation of the fluorescence intensity, as is commonly computed in fluorescence correlation spectroscopy (FCS). Clearly the average residence time is increased by feedback by roughly an order of magnitude, and decreased by anti-trapping. Nonetheless, molecules appear to not be held stably. At this point it is not clear whether the limitation is escape from the edges of the trap (due to the finite restoring force), or from the molecule going dark (due to a triplet state or photobleaching). Future work will examine other fluorophores with different photophysics.

5. Conclusion

We have demonstrated that by using a rotating laser focus and photon-by-photon phase sensitive detection it is possible to track the motion of individual fluorophores with sub-millisecond time resolution. This tracking information can be applied as feedback to keep a single fluorescent biomolecule within a small target region for extended observation. We expect that this device will prove invaluable in single-molecule studies of biomolecular function and interactions.

Acknowledgments

We thank So Yeon Kim and Stefanie Reissman for preparation of the labeled chaperonins. AEC acknowledges a Hertz Foundation Graduate Fellowship. This work was supported in part by the U. S. Department of Energy Grant No. DE-FG02-07ER15892, by the National Science Foundation Grant No. CHE-0554681, by the National Institutes of Health Grant No. 1R21-RR023149, by the NIH Roadmap for Medical Research Grant No. PN2-EY016525, and by the Stanford Nanofabrication Facility (a member of the National Nanotechnology Infrastructure Network) which is supported by the National Science Foundation Grant ECS-9731293.

#91292 - $15.00 USD Received 3 Jan 2008; revised 23 Apr 2008; accepted 30 Apr 2008; published 1 May 2008